THE UNIVERSITY *of* EDINBURGH

Edinburgh Research Explorer

Analysis of Planar Circular Interdigitated Electrodes for Electroporation

Citation for published version:

Link:
Link to publication record in Edinburgh Research Explorer

Document Version:
Peer reviewed version

OPEN ACCESS

Analysis of Planar Circular Interdigitated Electrodes for Electroporation

V. Novickij[1], A. Tabasnikov[2], S. Smith[2], A. Grainys[1], J. Novickij[1]

[1]Vilnius Gediminas Technical University, High Magnetic Field Institute, Vilnius, Lithuania
[2]University of Edinburgh, Scottish Microelectronics Centre, Edinburgh, UK

Abstract— in this work, designs for planar, interdigitated circular electrode structures for cell membrane permeabilization procedures are analysed using finite element method analysis. The generated electric field intensity, homogeneity and the Joule heating are evaluated. The optimal electrode configuration for successful transfection procedures is investigated. Based on the simulation results, an optimized design for the electrodes, suitable for the investigation of the permeabilization thresholds during electroporation is proposed. The Joule heating influence simulation results are validated experimentally.

Index Terms—electric field; permeabilization; transmembrane potential.

I. INTRODUCTION

Electroporation or electro-permeabilization is a biomedical technique to transfer molecules into cells based on the phenomena of the transient permeability increase of the cell membrane [1,2]. The increased permeability state of the cell is induced by a pulsed electric field treatment, which results in the formation of hydrophilic pores in the plasma membrane [3]. As a result the technique has found application for transport of molecules for which the membrane is initially impermeable [4].

However, the biophysical mechanisms of electroporation are still under debate, the lifetime of permeabilized state is being studied and the factors, which influence the treatment efficacy are also investigated [5]. Currently, there are reports, which show that the efficacy of electroporation and the viability rate of the cells are dependent on the electric field strength, pulse duration and pulse polarity [6-7]. However, dependent on the cell type, tissue or buffer the parameters vary, which creates a motivation for study of the permeabilization process in detail.

Several evaluation methodologies are available for investigation of the permeabilization process. The most common techniques include the application of fluorescently labeled molecules, measurement of conductivity changes due to changes in ionic concentrations and cell sorting techniques based on polarization such as dielectrophoresis (DEP) [8-10]. Generally, the most dominant method is the labeling of specific molecules and their injection into living cells. Typically, substances such as fluorescent dyes are loaded into the cells [11,12]. The cells are put into a cuvette with electrodes and after pulsing procedures the release or loading of the dye is observed [13, 14].

The majority of available electroporation systems use a standard 0.5 – 4 mm electrode gap cuvette with metal electrodes. One of the major issues using this method is the post-electroporation state observation due to the required cell handling from the cuvette to the microscope slide. Observation of the dye release dynamics is not possible during pulsing procedures. Therefore, possible implementations of planar microfluidic devices applicable for electroporation have been addressed [14 - 16]. Even though it is still difficult to study fast, nanoscale pore formation dynamics using real-time fluorescent microscopy, the planar electrode structures proved to be advantageous for electroporation experiments [14, 17]. The development of drug delivery embedded systems has started [14, 18]. However, the increased complexity of fabrication, small handling volumes and the electric field non-homogeneity issues are faced as a trade-off. Also, due to the same issues the scientific coverage of the planar electroporation is currently very limited. The novel and open problem of planar electrode application feasibility in electroporation still exists.

In 2011 Huang et al. proposed a planar interdigitated electrode structure for electroporation, which was applied for targeted delivery of siRNA [15]. The 100 µm electrode fingers with 500 µm electrode gap have been fabricated using patterned gold (300 nm thickness) on glass with chrome layer for gold adhesion [15]. The electrodes proved to be effective for planar electroporation. However, the analysis of electrode parameters such as thickness, electrode gap, finger width and their influence on the generated electric field intensity, field homogeneity and the generated Joule heating has not been performed.

In the current work, a feasibility study of circular improved planar interdigitated electrode structures that can be applied in electroporation is performed. The electric field strength, electric field distribution homogeneity and Joule heating due to the inevitable buffer resistivity are investigated by

V. Novickij, A. Grainys, J. Novickij are with the Vilnius Gediminas Technical University, High Magnetic Field Institute, Naugaduko 41, Vilnius, Lithuania (corresponding author: +37067410482; fax: +37052759501; e-mail: vitalij.novickij@vgtu.lt).

A. Tabasnikov, S. Smith are with University of Edinburgh, Scottish Microelectronics Centre, King's Building, Edinburgh, United Kingdom (e-mail: a.tabasnikov@ed.ac.uk).

simulation. The optimal dimensions of the electrodes, the values of electrode thickness, width and gap between the fingers are studied and recommendations for future developments are presented.

Application of finite element method (FEM) simulations and analytical approximation of the generated electric field in is a widely used methodology for investigation of the planar microelectrode structures [19-21]. Analytical approximations introduce additional parameter control and improved prototyping capabilities in the development of microchannels and electro-lysis devices [19, 20].

In this work the FEM simulations are applied for development of the improved version of interdigitated circular electrodes. In order to reduce the price of the final electrode structure and increase the simplicity of fabrication the copper laser etching technique has been applied. The proposed and fabricated electrodes are cheaper, easier to replicate and are suitable for generation of the electric field with high homogeneity, while the Joule heating is limited.

II. THEORY

Electroporation is based on the application of high voltage pulses in order to generate a high intensity electric field in a fixed volume cell buffer medium. When the cell is subjected to the electric field the membrane acts as a capacitor and a potential difference (transmembrane potential) is induced between the cytoplasm and the outer buffer medium [22]. The Schwan equation is typically used for theoretical description of the induced transmembrane potential in a spherical cell (at steady state) [23]:

$$V_T = 1.5 E r \cos\theta, \tag{1}$$

where E is the strength of the applied electric field, r is the radius of the cell, θ is the angle between the direction of the electric field and a point vector on the cell surface. When the potential difference threshold value is achieved the formation of transient nanoscale pores is observed.

As can be seen from Eq. 1 V_T is proportional to the electric field magnitude. Therefore, in order to achieve high repeatability of experiments and ensure equal electroporation effect to the cells in a buffer solution the precise generation of a homogeneous field must be implemented. As a rule a switch-controlled capacitor discharge through a cuvette with metal electrodes is used. The same methodology is applied when planar electrode structures are used as a load. The block diagram is shown in Figure 1. The planar electrodes can be mounted directly under a fluorescence microscope for real-time investigation of the dye release dynamics.

One of the biggest challenges with planar electrodes is the generation of a homogeneous electric field. Evaluation of the electric field distribution should always be performed. Estimation of the electric field in any given point for a 2D electrode array using an analytical solution can be based on the conformal mapping between Cartesian and cylindrical coordinates as proposed by Garcia and Clague [24]. The components of the electric field for a sequence of $(2n + 1)$

Fig. 1. Block diagram of the electroporation setup with planar electrodes

electrodes indexed using $i = [-n, (-n + 1) \dots (n - 1), n]$ and the corresponding applied potentials $\varphi_i(t)$ can be approximated as [24]:

$$
\begin{cases}
E_X(X,Y) = \dfrac{1}{\ln(G)\omega} \sum_{i=-n}^{n} \phi_i(t) \dfrac{u_i\left(\rho_i^2-1\right)^3\left(\rho_i^2+1\right)}{u_i^2\left(\rho_i^2-1\right)^4 + v^2\left(\rho_i^2+1\right)^4}, \\[4mm]
E_Y(X,Y) = \dfrac{1}{\ln(G)\omega} \sum_{i=-n}^{n} \phi_i(t) \dfrac{v\left(\rho_i^2-1\right)\left(\rho_i^2+1\right)^3}{u_i^2\left(\rho_i^2-1\right)^4 + v^2\left(\rho_i^2+1\right)^4},
\end{cases} \tag{2}
$$

where (X, Y) denotes a Cartesian coordinate system with an origin in the centre of interval $i = 0$; (u, v) are Cartesian coordinates normalized to half of electrode width ω; G is the radius to the zero field plane and ρ_i are radii from the origins of cylindrical intervals i to field point, both in cylindrical space. Radius G, at which potential is assumed to be zero depends on electrode configuration and can be found using [24]:

$$G = \frac{h}{\omega}\left(1 + \sqrt{1 + \frac{\omega^2}{h^2}}\right), \tag{3}$$

where h is the distance to the ground plane in Cartesian space.

In addition to electric field generation a Joule heating issue arises when current is flowing through the cell buffer [25]. However, performing thermal measurements in planar microfluidic structures is a complex task. Implementation of probes may disturb the properties of the setup and the treatment [26]. Therefore, analytical approximations are frequently applied. The amount of heat generated is proportional to the time over which the signal is applied, and the square of the current flowing through the medium:

$$Q_J \propto I^2 \tag{4}$$

However, evaluation of the temperature rise during each pulse also requires the knowledge of either the applied voltage or the resistivity of the medium. Evaluation of heat dissipation

requires information about the electrode geometry and convection parameters. In order to estimate all of these influencing factors it is convenient to apply finite element method analysis. Simulation is advantageous because it allows comparing the result in a wide range of parameters [27].

III.   FINITE ELEMENT METHOD ANALYSIS

Finite element method analysis has been performed using COMSOL Multiphysics software. Factors influencing both the electric field distribution and Joule heating effects were determined. In the simulations the free triangular mesh was used with a minimum and maximum finite element size of 0.5 µm and 0.37 mm, respectively. The minimum size is influenced by the geometry of the electrodes. The simulation includes an air container (4 mm x 10 mm), where the electrode structure is introduced (copper electrodes on FR-4 substrate). The thickness of FR-4 substrate is 1 mm. The 0.1 mm thick glass coverslip is used to cover the electrodes and the medium.

Implementation of glass or PDMS slides as a substrate is also applicable and does not have significant influence on the results of the simulation due to similar dielectric constants in the [3.5 – 6] range [28, 30]. The "electrical currents" and "Joule heating" physics have been chosen for simulation model in the COMSOL environment, which influenced the respective equations applied in the analysis.

The configuration of the electrodes and the respective typical voltage potential distribution in XY and YZ planes are shown in Figure 2. The use of sharp angles or corners in the electrode structures should be limited as much as possible to prevent high field gradients. Therefore, it was decided to use a circular interdigitated electrode structure. The summary of the simulation parameters is shown in Table 1.

As it is shown in Figure 2, the distribution of the electric potential is identical between the fingers or mirrored with a mirror plane in the centre of the array, therefore the analysis results of only two fingers will be presented further in the work. The electric field distribution between two electrode fingers when a potential of 100 V is applied is shown in Figure 3.

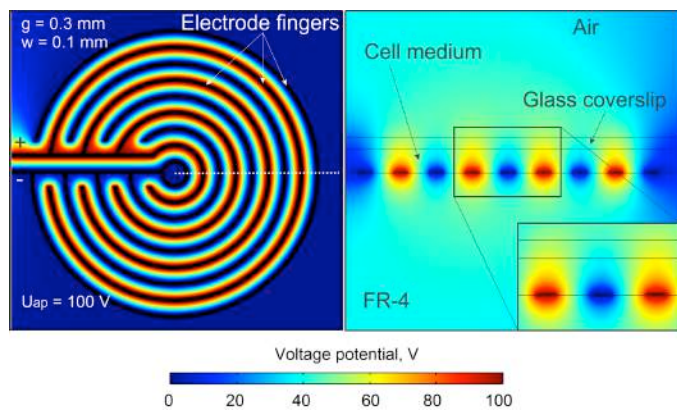As can be seen in Figure 3 the electric field is in the 1 –

TABLE I
SUMMARY OF SIMULATION PARAMETERS [28 - 30]

Denotation	Value range	Parameter
w	[20 µm – 200 µm]	Electrode width
g	[50 µm – 500 µm]	Electrode gap
a	[200 nm – 10 µm]	Electrode thickness
V_{ap}	[100 V – 300 V]	Applied voltage
ε_m	[70 – 80]	Medium permittivity
ε_G	[3.5 – 6]	FR-4/Glass permittivity
σ_m	[0.1 – 2 S/m]	Medium conductivity
σ_G	1×10^{-14} S/m	FR-4/Glass conductivity
σ_C	6×10^{7} S/m	Copper conductivity
C_{PC}	385 Jkg^{-1}K^{-1}	Copper specific heat capacity
k_C	400 Wm^{-1}K^{-1}	Copper thermal conductivity
C_{PG}	703 Jkg^{-1}K^{-1}	FR-4/Glass specific heat capacity
k_G	0.9 Wm^{-1}K^{-1}	FR-4/Glass thermal conductivity
C_{PM}	3990 Jkg^{-1}K^{-1}	Medium specific heat capacity
K_M	0.596 Wm^{-1}K^{-1}	Medium thermal conductivity
h	13.51	Convective cooling coefficient

3 kV/cm range, which is applicable for reversible electroporation procedures [1,3]. However, the non-homogeneity of the electric field distribution will negatively affect the biological experiments, introducing additional uncertainty to the results. As shown in Figure 3 the region with high electric field homogeneity (557 – 650 µm) is suitable for planar electroporation (E = 2 kV/cm), however it is convenient to increase the segment as much as possible. A trade-off between the effective volume of effect and the homogeneity of the field must be reached. In order to address this issue the influence of electrode gap and thickness on the distribution of the electric field was studied. The dependence of the homogeneity segment on the electrode gap is shown in Figure 4. The segment has been determined as the distance between two points in the same plane, where the amplitude of the electric field does not vary more than 20%, 5% and 1%
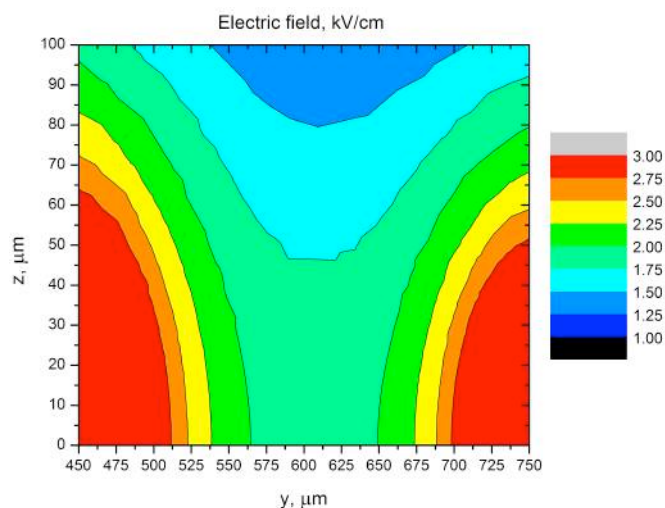

Fig. 2.   Typical voltage potential distribution of circular interdigitated electrodes in XY plane (Left) and YZ plane (Right)

Fig. 3. The YZ plane electric field distribution when, g = 0.3 mm, w = 0.1 mm, V_{ap} = 100 V.
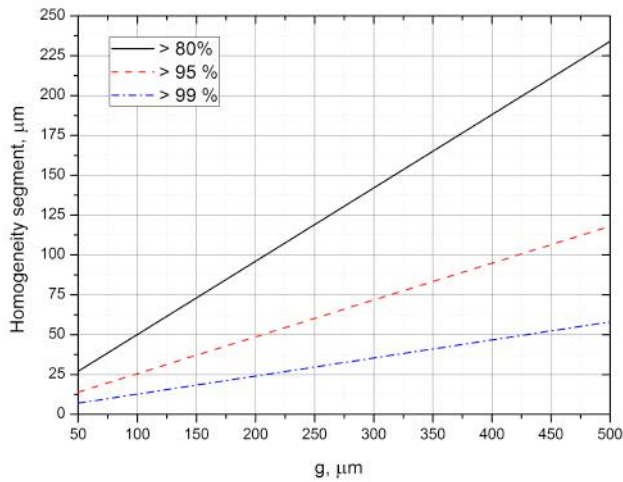
Fig. 4. The dependence of the homogeneity segment versus the electrode gap

from the minimum value. The results indicate that a wider gap between the electrodes is advantageous for higher XY plane electric field homogeneity.

The minimum acceptable size of the required homogeneous region is limited by the size of the cells and the complexity of determination of the position of the cells in a homogenous region, which influences the uncertainty of the results. Due to dielectrophoretic movement of cells during pulsing the electrodes with the 50 µm gap are hardly applicable. At the opposite end of the scale, the 500 µm gap electrodes offer the widest homogeneity region, however as a trade-off the voltage applied would be significantly higher to achieve the same magnitude of electric field. If a <20% non-homogeneity rate is acceptable, the 250 – 350 µm gap electrodes are optimal for cells <50 µm, providing a sufficient reserve in area for cell movement during pulsing. The acceptable electric field non-homogeneity rate should be selected based on the cell size, type and the specifics of the experiments.

In order to evaluate the influence of metal layer thickness on the electric field distribution, a has been varied from

0.2 µm to 10 µm. The results are applicable for electrodes fabricated by metal deposition using photolithography and for PCB boards fabricated using etching techniques. The dependence of the electric field amplitude on the electrode thickness in both the XY and YZ planes is shown in Figure 5. Only the marginal cases of electrode thickness are shown.

As it can be seen in Figure 5 the alteration of thickness in the 0.2 µm – 10 µm range has no significant influence on the electric field homogeneity. However, the magnitude of the field is increased by 9% in the $a = 10$ µm case compared to the $a = 0.2$ µm configuration. Based on the result it was concluded that the applicability of electrodes is independent from the type of the fabrication process that was used.

Apart from the electric field generation the Joule heating issue arises when the current is flowing through the cell buffer. A simulation has been performed when a 100 V pulse of 500 µs duration was applied to the electrodes. The results of the simulation are shown in Figure 6.

As can be seen in Figure 6 a temperature rise of up to 5 °C is expected after a 500 µs pulse. Several seconds are required for the cell medium to cool down. The electroporation experiments as a rule are performed in room temperature, however even though the thermal influence due to pulsing is short term, temperatures above 37 °C could distort the experimental results. Therefore, maximum pulse number and repetitive frequency limitations must be introduced for each specific electrode configuration.

Also the Joule heating can be minimized if a high-impedance cell medium is used. However, cell medium type limitation will negatively influence the applicability of the electrodes, therefore all of the simulations have been performed with highly conductive medium (Table 1).

Based on the simulations it was decided that the circular interdigitated electrodes configuration is applicable for the electroporation studies. The structure offers separate instances with the same or mirrored electric field distribution, which implies that better statistical analysis of the experimental results can be performed. The homogeneity region can be
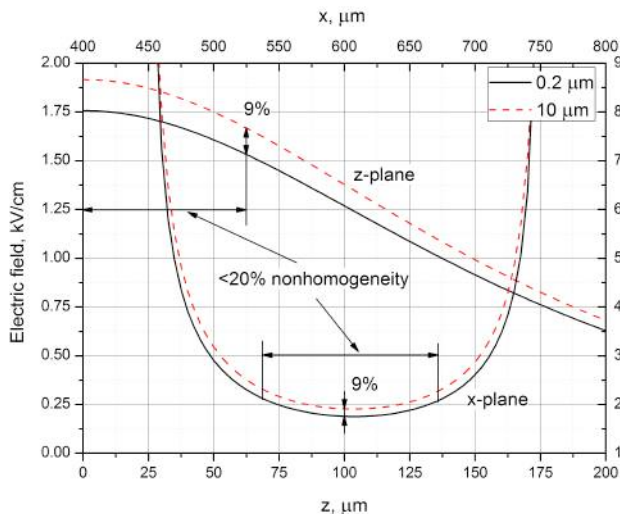

Fig. 5. The dependence of the electric field amplitude on the electrode thickness in the XY (height above electrodes: 10 µm) and YZ (evaluation point position x: 600 µm) planes
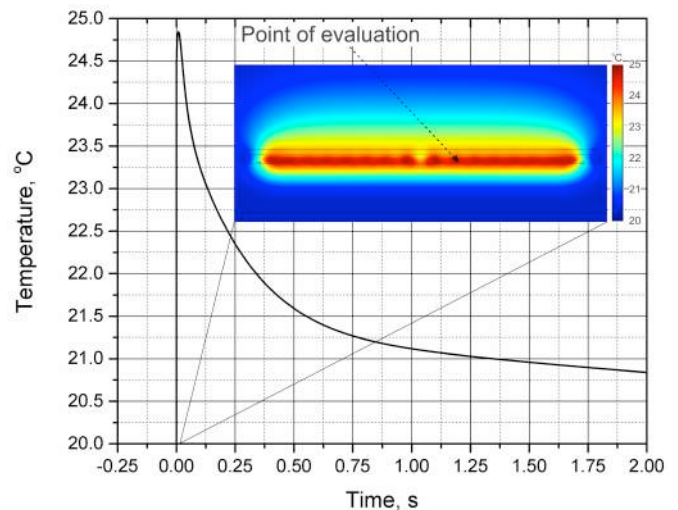

Fig. 6. Temperature rise in the cell buffer due to Joule heating after a 500 µs pulse, when $g = 0.3$ mm, $w = 0.1$ mm, $V_{ap} = 100$ V.

controlled by the alteration of the gap between electrodes.

IV.   ELECTRODE DESIGN

It was decided that the electrode geometry with 300 µm gap is optimal due to the relatively wide >130 µm homogeneity region (>80% homogeneity, Figure 4). The width of the electrode fingers is 100 µm. The design of a circular electrode array with 6 set of electrode is shown in Figure 7.

The structure has been fabricated on a PCB copper board using laser etching. The thickness of the copper layer is equal to 7 µm. The dimensions of the final chip are 5.5 cm x 3.3 cm. One of the biggest advantages of using FR-4 and etching to form the electrodes is the simplicity and low price of the production. However, certain limitations for fluorescence study will apply, such as a requirement of a direct light source for fluorescence excitation. For the inverted fluorescence microscopy the glass or PDMS substrates are desirable.

The Joule heating influence has been evaluated experimentally. The developed electrodes have been connected to a controlled width square wave electric pulse generator and the conductivity change measurement methodology has been applied [31]. As a medium distilled water (high impedance) and 0.9% NaCl solution (low impedance) have been used. Based on the difference in the pulsed current during the pulse the conductivity change and the respective temperature changes have been evaluated. The 100 µs and 500 µs pulses were used. The results are presented in Figure 8.

As shown in Figure 8 the difference in pulsed current during 100 µs pulse is <1%, which implies that the

Fig. 8. Voltage drop change due to the cell medium conductivity change, where I_0 is the current in the beginning of the pulse.

temperature rise can be neglected. However, during the longer pulse, there 8.9% difference is present, which corresponds to 3-4 °C temperature rise [32]. The experimental data is in acceptable compliance with the simulation results.

V.   CONCLUSION

Application of planar electrodes in electroporation allows real-time microscopic analysis, which benefits studies focused on an investigation of the transmembrane potential and permeabilization dynamics. In this study using FEM it has been shown that, in order to acquire a homogeneous region of electric field a trade-off between the electrode gap size and the resultant generated homogeneous electric field region must be made. The thickness of the electrodes does not have significant influence on the homogeneity, which introduces additional freedom for fabrication process. Based on the FEM analysis a planar interdigitated electrode structure has been designed and fabricated as a printed circuit board using direct laser etching. Future studies will involve application of the developed structure in electroporation experiments for investigation of the permeabilization dynamics of biological cells. For long term experiments gold electroplating is advised in order to improve the biocompatibility of the electrodes.
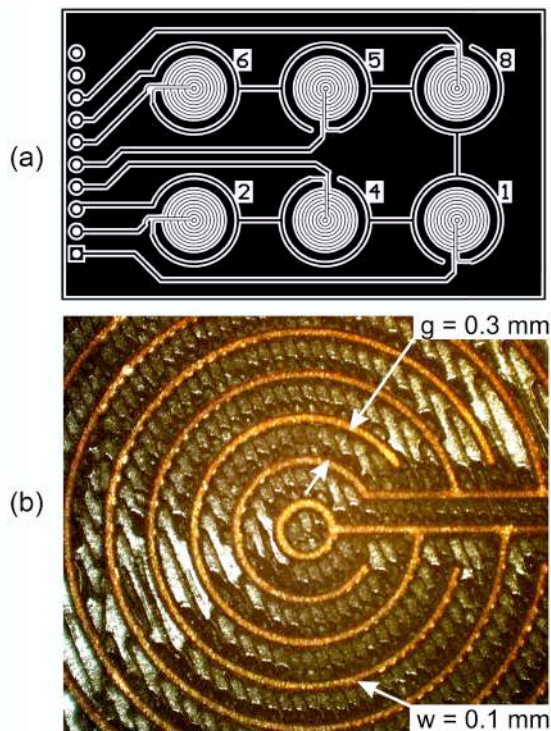

Fig. 7.   The developed interdigitated electrode structure based on FEM simulation results, where a) the chip with an array of electrodes; b) the photograph of the copper electrodes etched on FR-4 epoxy laminate
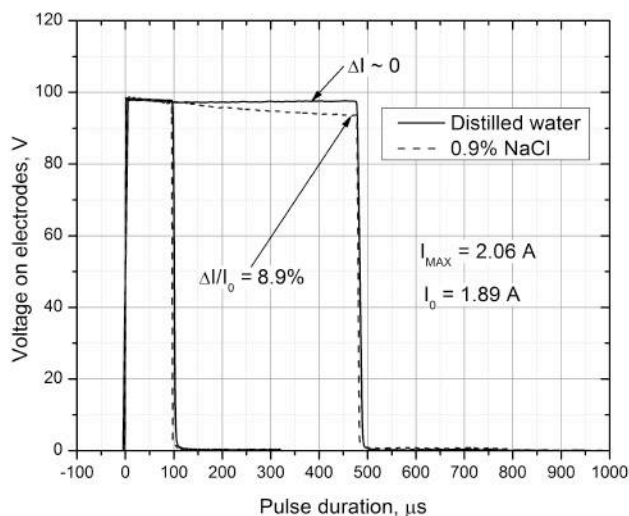
REFERENCES

[1]   S. B. Dev, D. P. Rabussay, G. Widera, and G. A. Hofmann, "Medical applications of electroporation," *IEEE Trans. on Plasma Sci.,* vol. 28, pp. 206–223, 2000.

[2]   D. Skuk, M. Goulet and J. P. Tremblay, "Electroporation as a method to induce myofiber regeneration and increase the engraftment of myogenic cells in skeletal muscles of primates", *Journal of Neuropathology and Experimental Neurology*, vol. 72, no. 8, pp. 723–734, 2013.

[3]   T. Kotnik, P. Kramar, G. Pucihar, D. Miklavcic and M. Tarek, "Cell membrane electroporation - part 1: The phenomenon," IEEE Elect. Insul. Mag., vol. 28, no. 5, pp. 14 – 23, 2012.

[4]   K. Cahill, "Cell-penetrating peptides, electroporation and drug delivery", *IET Systems Biology,* vol. 4, no. 6, pp. 367–378, 2010.

[5]   P. J. Canatella, J. F. Karr, J. A. Petros, M. R. Prausnitz, "Quantitative study of electroporation-mediated molecular uptake and cell viability," *Biophys J*., vol. 80, no. 2, pp. 755-764, 2001.

[6] Y. Zhan, C. Sun, Z. Cao, N. Bao, J. Xing and C. Lu, "Release of Intracellular Proteins by Electroporation with Preserved Cell Viability," *Analytical Chemistry,* vol. 84, no. 19, pp. 8102-8105, 2012.

[7] M. B. Sano, C. B. Arena, M. R. DeWitt, D. Saur, R. V. Davalos, "In-vitro bipolar nano-and microsecond electro-pulse bursts for irreversible electroporation therapies," *Bioelectrochemistry*, vol. 100, pp. 69-79, 2014.

[8] M. Sustarsic, A. Plochowietz, L. Aigrain, Y. Yuzenkova, N. Zenkin, A. Kapanidis, "Optimized delivery of fluorescently labeled proteins in live bacteria using electroporation," *Histochemistry and Cell Biology,* vol. 142, no. 1, pp. 113-124, 2014.

[9] A. Ivorra, B. Al-Sakere, B. Rubinsky, L. M. Mir, "In vivo electrical conductivity measurements during and after tumor electroporation: conductivity changes reflect the treatment outcome," *Phys. Med. Biol.,* vol. 54, no. 19, pp. 5949 – 5963, 2009.

[10] C. H. Wang, Y. H. Lee, H. T. Kuo, W. F. Liang, W. J. Li, G. B. Lee, "Dielectrophoretically-assisted electroporation using light-activated virtual microelectrodes for multiple DNA transfection," *Lab Chip*, vol. 14, pp. 592 – 601, 2014.

[11] C. Rosazza, A. Buntz, T. Riesz, D. Woll, A. Zumbusch, M. P. Rols, "Intracellular Tracking of Single-plasmid DNA Particles After Delivery by Electroporation," *Mol. Ther.*, vol. 21, no. 12, pp. 2217-2226, 2013.

[12] H. Tsugiyama, C. Okimura, T. Mizuno, Y. Iwadate, "Electroporation of adherent cells with low sample volumes on a microscope stage," *J. Exp. Biol.*, vol. 216, pp. 3591 – 3598, 2013.

[13] A. Stirke et al., "Electric field-induced effects on yeast cell wall permeabilization," *Bioelectromagnetics*, vol. 35, no. 2, pp. 136 – 144, 2014.

[14] T. Geng, C. Lu, "Microfluidic electroporation for cellular analysis and delivery," *Lab Chip*, vol. 13, pp. 3803 – 3821, 2013.

[15] H. Huang et al., "An efficient and high-throughput electroporation microchip applicable for siRNA delivery," *Lab on Chip*, vol. 11, pp. 163-172, 2011.

[16] Y. Xu, H. Yao, L. Wang, J. Cheng, "The construction of an individually addressable cell array for selective patterning and electroporation," *Lab on Chip*, vol. 11, no. 14, pp. 2417 – 2423, 2011.

[17] J. Cemazar, D. Miklavcic, T. Kotnik, "Microfluidic devices for manipulation, modification and characterization of biological cells in electric fields – a review," *INFORM MIDEM*, vol. 43, no. 3, pp. 143-161, 2013.

[18] S. Kaur, "How are the embedded chips going to affect out lives?," *IETE Techical Review*, vol. 20, no. 2, pp. 101 – 104, 2012.

[19] B. I. Morshed, M. Shams, T. Mussivand, "Analysis of Electric Fields Inside Microchannels and Single Cell Electrical Lysis with Microfluidic Device," *Micromachines*, vol 4, no. 2, pp. 243-256, 2013.

[20] A. Jenkins, C. P. Chen, S. Spearing, L. A. Monaco, A. Steele, G. Flores, "Design and modeling of a microfluidic electro-lysis device with controlling plates," *Proceedings of the 2006 International MEMS Conference*, May 9 – 12, Singapore, pp. 620-625, 2006.

[21] P. Linderholm, U. Seger, P. Renaud, "Analytical expression for electrical field between two facing strip electrodes in microchannel," *Electron. Lett.*, vol. 42, pp. 145-146, 2006.

[22] L. Chengxiang, Y. Chenguo, S. Caixin, G. Fei, Z. Wei, X. Zhengai, "Dependence on electric field intensities of cell biological effects induced by microsecond pulsed electric fields", *IEEE Trans. Dielectr. Electr. Insul.*, vol. 18, no. 6, pp. 2083–2088, 2011.

[23] P. Marszalek, D. S. Liu, T. Y. Tsong, "Schwan equation and transmembrane potential induced by alternating electric field," *Biophys J.*, vol. 58, no. 4, pp. 1053 – 1058, 1990.

[24] M. Garcia, D. Clague, "The 2D electric field above a planar sequence of independent strip electrodes," *J. Phys. D: Appl. Phys.*, vol. 33, pp. 1747 – 1755, 2000.

[25] R. V. Davalos, B. Rubinsky, "Temperature consideration during irreversible electroporation," *Int. J. Heat Mass Transfer*, vol. 51, pp. 5617-5622, 2008.

[26] B. Rosal, C. Sun, D. N. Loufakis, C. Lu, D. Jaque, "Thermal loading in flow-through electroporation microfluidic devices," *Lab Chip*, vol. 13, pp. 3119 – 3127, 2013.

[27] H. Zafar, M. Zuhairi, D. Harle, I. Andonovic, "A review of techniques for the analysis of simulation output," *IETE Technical Review*, vol. 29, no. 3, pp. 223-228, 2012.

[28] M. Pavlin, M. Kanduser, M. Rebersek, G. Pucihar, F. X. Hart, R. Magjarevic, D. Miklavcic, "Effect of cell electroporation on the conductivity of a cell suspension," *Biophys J*, vol. 88, pp. 4378-4390, 2005.

[29] J. Kuncova-Kallio, P. J. Kallio, "PDMS and its suitability for analytical microfluidic devices," *Proceedings of the 28th IEEE EMBS International Conference*, Aug 30 – Sept 3, pp. 2486 – 2489, 2006.

[30] V. Gupta, P. Sahoo, "Performance improvement of microstrip patch antenna using left-handed metamaterial," *IJRECT 2014*, vol. 1, no. 1, pp. 46 – 49, 2014.

[31] V. Novickij, A. Grainys, J. Novickij, S. Tolvaisiene, S. Markovskaja, "Compact Electro-Permeabilization System for Controlled Treatment of Biological Cells and Cell Medium Conductivity Change Measurement," *Measurement Science Review*, vol. 14, no .5 pp. 279-284, 2014.

[32] M. Hayashi, "Temperature-electrical conductivity relation of water for environmental monitoring and geophysical data inversion," *Environ Monit Assess.*, vol. 96, pp. 119-128, 2004.

Vitalij Novickij received his BEng degree in Electronics and Electrical Engineering from Vilnius Gediminas Technical University. He received MSc degree in Bioelectronics from University of Edinburgh in 2011. From 2012 he is pursuing PhD degree in the field of electronics and electrical engineering. His current research interests include pulsed power application in biology including the study of the effects of the pulsed electric and magnetic fields.

Aleksandr Tabasnikov received his BEng degree in Electronics and Electrical Engineering from Vilnius Gediminas Technical University in 2010. He received MSc degree in Bioelectronics from the University of Edinburgh in 2011. He is currently a PhD student in the Institute for Integrated Micro and Nano Systems, the University of Edinburgh. His research interests include thin film fabrication and processing, high temperature sensors and transducers, post-processing and smart microsystems.

Stewart Smith received the B.Eng. (hons) degree in Electronics and Electrical Engineering in 1997 and the Ph.D. degree in 2003 from the University of Edinburgh, Scotland, UK. Stewart is a Lecturer in Electronics with the School of Engineering at the University of Edinburgh. His research interests include the design and fabrication of biological and medical microsystems, integration of novel technologies with CMOS and test structures for microsystem fabrication processes. He was recently appointed to the Royal Society of Edinburgh, Young Academy of Scotland and is an irregular contributor to the YAS blog http://researchtheheadlines.org.

Audrius Grainys received his MSc degree from Vilnius Gediminas Technical University. He received his doctoral degree in the Electronics and Electrical Engineering in 2014. From 2012 he is working as a researcher in the High Magnetic Fields Institute in Vilnius Gediminas Technical University. His current research interests include pulsed power application in biology and material sciences, generation and measurement of pulsed magnetic and electric fields.

Jurij Novickij received doctoral degree in the field of electronics and electrical engineering from the Vilnius Gediminas Technical University in 2000. Now he is a professor at Vilnius Gediminas Technical University and the director of the High Magnetic Field Institute. His current research interests include generation, application and measurement of pulsed magnetic and electric fields.